ORIGINAL ARTICLE

Deficiency of brain structural sub-network underlying post-ischaemic stroke apathy

S. Yang[a,b,*], P. Hua[c,*], X. Shang[b], Z. Cui[d], S. Zhong[d], G. Gong[d] and G. William Humphreys[a]

[a]*Department of Experimental Psychology, University of Oxford, Oxford, UK;* [b]*Department of Neurology, Guangzhou First People's Hospital, Guangzhou Medical University, Guangzhou;* [c]*Department of Cadio-vascular surgery, Sun Yat-sen Memorial Hospital, Sun Yat-sen University, Guangzhou; and* [d]*State Key Laboratory of Cognitive Neuroscience and Learning & IDG/McGovern Institute for Brain Research, Beijing Normal University, Beijing, China*

Keywords:
apathy, brain network, diffusion tensor imaging, stroke, white matter

Received 26 May 2014
Accepted 25 August 2014

European Journal of Neurology 2015, **22:** 341–347

doi:10.1111/ene.12575

Background and purpose: This study aimed to reveal the structural basis of post-ischaemic stroke apathy, especially in relation to disruptions in structural connectivity.

Methods: Eighty-eight participants were included. The Apathy Evaluation Scale, clinician version, was used to characterize the severity of apathy. Diffusion tensor imaging tractography was used to examine white matter integrity and to reconstruct white matter networks using 90 nodes based on the automated anatomical labeling atlas. The degree for each node was extracted to determine the relationship to the severity of apathy.

Results: Apathy was not significantly associated with damage to any single brain region. The degrees of 24 nodes (limbic system, three nodes; frontal lobe, six; basal ganglia, two; temporal lobe, three; parietal lobe, three; insula, two; occipital lobe, five) were significantly correlated to the Apathy Evaluation Scale scores. These 24 nodes constituted an apathy-related sub-network and its global and local efficiencies were negatively correlated with apathy levels (global, $r = -0.54$, $P < 0.01$; local, $r = -0.64$, $P < 0.01$). Multivariate logistic regression indicated that decreased global efficiency of this sub-network was an independent risk factor for apathy (odds ratio 0.03, 95% confidence interval 0.01–0.04, $P = 0.007$). Efficiencies of the non-apathy-related sub-network (the remaining 66 nodes) did not correlate or predict the presence of apathy.

Conclusions: Post-stroke apathy is not due to the dysfunction of a single region or circuit. Rather, it results from disconnection of a complex sub-network of brain regions. This provides new insights into the neuroanatomical basis of post-stroke apathy.

Apathy can be defined as a lack of motivation that is not attributable to diminished levels of consciousness, emotional distress or cognitive impairment [1], which appears in about 35% of stroke patients [2]. The few neuroimaging studies conducted on the disorder indicate that damage within particular brain regions, such as the frontal lobe, basal ganglia, thalamus and temporal lobe [3,4], is associated with apathetic symptoms following stroke. However, a meta-analysis showed no clear association between apathy and any specific lesion location [2]. Prior studies have focused primarily on regional differences and local brain lesions, but whether there is a breakdown in brain-network interactions has not been established. Here, whether this putatively independent, affective symptom of stroke [5] is linked to a specific neuroanatomical network was assessed.

Diffusion tensor imaging (DTI) tractography is a non-invasive technique to virtually reconstruct white matter (WM) pathways in living people [6]. Recently,

Correspondence: S. Yang, Department of Experimental Psychology, University of Oxford, 9 South Parks Road, Oxford OX1 3UD, UK (tel.: +44 (0) 1865 618631; fax: +44 (0) 1865 310447; e-mail: yangsongran@126.com) and G. Gong, State Key Laboratory of Cognitive Neuroscience and Learning, Beijing Normal University, Beijing 100875, China (tel.: +86 10 58804678; fax: +86 10 58806154; e-mail: gaolang.gong@bnu.edu.cn).
*These authors contributed equally to the paper.

graph analyses have been applied to neural network organization to model structural and functional connections from the perspective of neuronal topological organization [7]. Here, the brain lesions and topological characteristics of WM networks in a group of participants who survived stroke were explored. Specifically, it was hypothesized that disruption of connectivity within a specific brain sub-network is associated with symptoms of apathy following stroke. DTI tractography was employed to construct WM networks within the brain, and graph analyses were used to quantify the topological properties of the constructed networks.

Methods

Participants

Ischaemic stroke patients admitted to Guangzhou First People's Hospital between January 2013 and December 2013 were included. All participants satisfied the following inclusion criteria: (i) the National Institutes of Health Stroke Scale (NIHSS) score was not higher than 6; (ii) a series of brain magnetic resonance imaging (MRI) scans, including T1, T2, fluid-attenuated inversion-recovery (FLAIR) and DTI taken within 7 days of stroke onset were available and of good quality; (iii) participants were conscious and cooperated with the evaluation scales. Participants who had a history of schizophrenia, depression, anxiety, dementia, severe drinking (>42 drinks per week) or drug abuse or a family history of mental disorders were excluded.

The Apathy Evaluation Scale, clinician version (AES-C), was used to quantify the level of apathy of each participant [1,8] whilst an experienced neuropsychologist carried out the clinical diagnosis for apathy, within 1 month after the stroke. The diagnostic criteria for this study were based on the Marin scale [1] and Robert *et al.* [9].

Fifty-four participants without apathy (36 males, age 67.8 $\pm$ 10.3 years) and 34 participants with apathy (28 males, age 68.7 $\pm$ 8.7 years) were included in the study. NIHSS scores were recorded on admission. The Hamilton Depression Rating Scale 24 item (HDRS-24), the Mini Mental State Examination (MMSE) and the Barthel Index were also evaluated within 1 month of stroke onset. Informed written consent was obtained from each participant, and the research protocol was approved by the Ethics Committee of Guangzhou First People's Hospital.

Acquisition of imaging data

MRI scans were acquired using a Siemens Verio 3.0-T scanner (Siemens, Erlangen, Germany). The T1-weighted images were scanned with the following parameters: repetition time 1900 ms, echo time 3.44 ms, inversion time 900 ms, flip angle 9° and voxel size $1 \times 1 \times 1$ mm^3. The FLAIR T2 images were scanned with a slice thickness of 5 mm. Each DTI scan consisted of 30 diffusion-weighted volumes with a b value of 1000 s/mm^2 and one volume without diffusion weighting (i.e. b_0 image), with slice thickness 3 mm and no gap.

Structural MRI data preprocessing

The structural sequences were co-registered linearly in individual space with six degrees of freedom [10]. Then, by referring to the FLAIR T2 images, an experienced radiologist manually drew the lesion contours slice by slice for each participant. Next, the nonlinear registration method was applied to align the individual structural images to the Montreal Neurological Institute (MNI) standard space with a resliced voxel size of $1 \times 1 \times 1$ mm^3. The location of the lesion was also transformed into MNI space.

Whole brain statistical parametric mapping

The relationship between tissue damage and apathy was explored using Statistical Parametric Mapping 8 (SPM8) (Wellcome Department of Cognitive Neurology, London, UK). To exclude confounding factors, age, gender, lesion size, HDRS score and MMSE score were included in the analysis as covariates. Statistical criteria were set at uncorrected $P < 0.001$ with a cluster size >100.

Construction of brain WM networks

The pipeline software PANDA was used to construct the brain WM network [11]. Brain areas (except for the pons and cerebellum) were parceled into 90 regions according to the Automated Anatomical Labeling atlas [12] and were used to define the nodes of the WM network. Fiber assignment by continuous tracking [13] was used to perform deterministic fiber tracking [14] by seeding from voxels with fractional anisotropy values >0.2. The edges, which linked pairs of brain nodes/regions, were extracted from the fibers with the two end-points located in their respective masks. Thus a network matrix for each subject was generated with each row/column representing a brain node and each element representing the averaged fractional anisotropy of the fibers linking the nodes.

The degree of each node was quantified as the number of edges connected to the node [15] and was used here as a reliable index to reflect the regional

connectivity. The topological properties of the associated brain networks were analyzed using the GRETNA toolbox [16]. The small-world behavior was assessed by the coefficient σ [17] which uses a ratio of network clustering and path length to contrast with the same metrics from an equivalent random network. For $\sigma > 1$ a network is considered to have small-world behavior. Global and local efficiencies were evaluated for whole brain and identified local networks, respectively. Global efficiency indicates how efficiently information is communicated within a network at the global level. Local efficiency indicates how efficiently information transfers within the neighbors of a given node when that node is removed, and represents how tolerant the complex network is [15].

Subdivision of the whole brain network

A partial correlation analysis was performed between the degree of each node and the AES-C score, controlling for age, gender, lesion size, HDRS score and MMSE score. Multiple comparisons were corrected using the false discovery ratio (FDR) method (corrected $P < 0.05$). Those nodes whose degrees correlated with the AES-C score were selected to build an apathy-related sub-network, whilst the others were used to construct a sub-network unrelated to apathy. Small-world behavior and the global and local efficiencies of the sub-networks were further analyzed.

Assessment of the unique contribution of the sub-network identified for apathy

After controlling for age, gender, lesion size, HDRS score and MMSE score, partial correlation analysis between the AES-C scores and the efficiencies of the identified sub-networks was performed. Variables with $P < 0.20$ in univariate logistic regression analysis were included in multivariate logistic regression models with conditional forward selection to assess the unique contribution of the identified sub-network to the presence of apathy. All statistical assessments were two-tailed and statistical significance was set at $P < 0.05$. Statistical analyses were performed using SPSS 15.0 statistical software (SPSS Inc., Chicago, IL, USA).

Results

None of the demographic characteristics differed between the apathetic and non-apathetic groups, as summarized in Table 1.

Table 1 Summary of baseline characteristics for the 88 stroke cases

	Apathy group (n = 34)	Non-apathy group (n = 54)	P value
Age (year)	68.7 ± 8.7	67.8 ± 10.3	0.665
Gender, n (%)			
Male	28 (82.4)	36 (66.7)	0.142
Female	6 (17.6)	18 (33.3)	0.142
Education (years)	8.1 ± 3.0	8.6 ± 5.0	0.589
Lesion size (cm^3)	10.7 ± 11.4	6.7 ± 8.5	0.088
HDRS score	9.9 ± 4.3	8.5 ± 2.4	0.087
NIHSS score	1.8 ± 1.9	1.2 ± 1.4	0.077
MMSE score	26.1 ± 2.2	26.9 ± 2.1	0.102
BI	73.8 ± 16.2	79.1 ± 13.3	0.102

BI, Barthel Index. Data are displayed as mean ± standard deviation and as number (percentage).

SPM results for lesioned areas associated with apathy

Figure 1 shows the SPM results for lesion areas associated with post-stroke apathy at the $P < 0.001$ level (uncorrected). One cluster was detected with peak voxels in the right external capsule and right superior corona radiata. However, this finding did not survive correction for multiple comparisons (FDR method).

Brain regions showing significant correlations between nodal degree and AES-C scores

Intriguingly, 24 nodes (limbic system, three nodes; frontal lobe, six; basal ganglia, two; temporal lobe, three; parietal lobe, three; insula, two; occipital lobe, five) with degrees that were significantly correlated with AES-C score were found (Table 2). The whole brain network can therefore be divided into a sub-network composed of 24 apathy-related nodes (i.e.

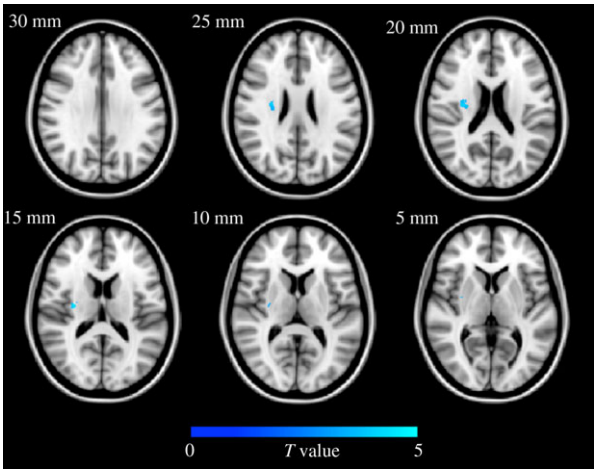

Figure 1 Positive brain regions from the SPM lesion analysis. The color map indicates positive clusters in the lesion analysis ($P < 0.001$, uncorrected; cluster size >100 voxels).

Table 2 Brain regions showing significant correlations between nodal degree and AES-C scores

Location	Brain region	Nodal degree (r)	Nodal degree (P)
Frontal lobe (n = 6)	Precentral_R	−0.507	<0.001
	Frontal_Inf_Tri_R	−0.305	0.005
	Frontal_Inf_Orb_L	−0.334	0.002
	Frontal_Inf_Orb_R	−0.336	0.002
	Supp_Motor_Area_L	−0.308	0.005
	Frontal_Med_Orb_L	−0.302	0.006
Insula (n = 2)	Insula_L	−0.288	0.008
	Insula_R	−0.377	<0.001
Limbic system (n = 3)	Cingulum_Post_L	−0.312	0.004
	Cingulum_Post_R	−0.300	0.006
	Hippocampus_L	−0.296	0.007
Parietal lobe (n = 3)	SupraMarginal_R	−0.502	<0.001
	Precuneus_R	−0.388	<0.001
	Paracentral_Lobule_R	−0.296	0.007
Basal ganglia (n = 2)	Putamen_R	−0.316	0.004
	Thalamus_R	−0.307	0.005
Occipital lobe (n = 5)	Calcarine_R	−0.479	<0.001
	Cuneus_R	−0.282	0.010
	Lingual_R	−0.371	0.001
	Occipital_Sup_R	−0.340	0.002
	Occipital_Inf_L	−0.331	0.002
Temporal lobe (n = 3)	Temporal_Sup_R	−0.325	0.003
	Temporal_Pole_Sup_L	−0.314	0.004
	Temporal_Pole_Sup_R	−0.440	<0.001

The FDR correction method (the corrected $P < 0.05$ corresponds to an uncorrected $P < 0.012$) was applied. The full names of the abbreviations are listed in Table S1.

apathy-related sub-network) and one formed by the other 66 nodes (i.e. apathy-unrelated sub-network) (Fig. 2).

The contribution of identified sub-network for post-stroke apathy

Using graph theoretical analyses, the whole brain WM networks, the apathy-related sub-network and the apathy-unrelated sub-network showed high σ values (2.57 ± 0.97, 2.25 ± 0.85 and 2.89 ± 0.77 respectively). In particular, both local and global efficiencies for the apathy-related sub-network were significantly negatively correlated with AES-C scores ($r = -0.54$, $P < 0.01$; $r = -0.64$, $P < 0.01$), whilst the efficiencies of the apathy-unrelated sub-network were not ($r = -0.19$, $P = 0.08$; $r = -0.15$, $P = 0.17$).

Table 3 presents the results of the logistic regression analyses conducted to determine the factors potentially associated with the presence of apathy. Multivariate logistic regression indicated that decreased global efficiency in the apathy-related sub-network (odds ratio 0.03, 95% confidence interval 0.01–0.04, $P = 0.007$) was an independent risk factor for the presence of apathy.

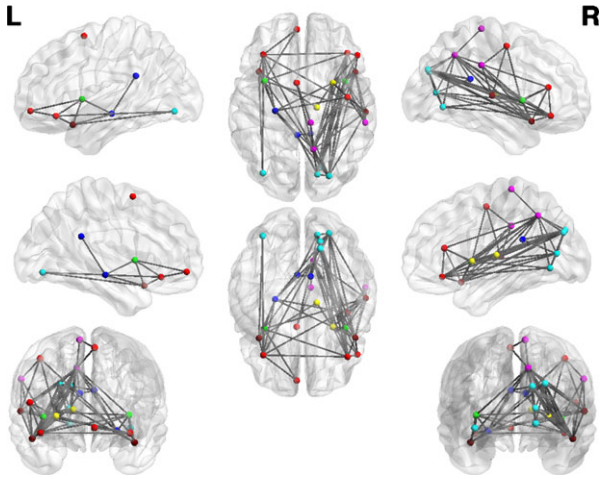

Figure 2 The apathy-related sub-network. Each ball denotes a brain node: red for frontal cortex, yellow for basal ganglia, violet for parietal regions, dark red for temporal cortex, dark blue for the limbic system, blue for occipital cortex and green for insula. Each line denotes a connection between the nodes. The image was displayed by using Brainnet viewer [18].

Discussion

To the best of our knowledge, this is the first study exploring the neuronal basis of post-stroke apathy from the perspective of WM connectivity. Our findings can be briefly summarized as follows: (i) 24 brain regions were identified to be significantly correlated with post-stroke apathy levels; (ii) the global efficiency of this apathy-related sub-network was an independent risk factor for post-stroke apathy.

Brain lesions in the right external capsule and right superior corona radiata were associated with the presence of apathy, although this finding did not survive FDR correction. After stroke, the effects on WM tract integrity caused by the primary lesion can be both local and distal [19], meaning that local lesions rarely reflect the total damage to the brain circuitry.

The relationship between brain region connectivity and severity of apathy was further analyzed. Stuss *et al.* [20] argued that apathetic syndromes can be divided into three subtypes: emotional, cognitive and behavioral. Emotional blunting can be thought of as the main characteristic of the emotional subtype, reflecting a decreased impact of emotion and affect on ongoing or forthcoming behaviors [21]. Evidence shows that lesions of orbital-medial prefrontal cortex lead to emotional blunting, perhaps through damage to reward-related processing circuits [22]. Here it is predicted that disconnectivity of this region is also associated with emotional aspects of apathy. Our results support this assertion by identifying nodes within the bilateral orbital part of the inferior frontal gyrus and the left orbital part of the

Table 3 Determinants of significant risk factors associated with post-stroke apathy (n = 88)

	Univariate		Multivariate	
	OR (95% CI)	*P* value	OR (95% CI)	*P* value
Age (years)	1.01 (0.97, 1.06)	0.661		
Female	0.43 (0.15, 1.22)	0.113		
Education (years)	0.97 (0.88, 1.08)	0.584		
Lesion size (mm^3)	1.00 (1.00, 1.00)	0.076		
NIHSS score	1.29 (0.99, 1.68)	0.062		
Barthel Index	0.98 (0.95, 1.00)	0.106		
HDRS score	1.14 (1.00, 1.31)	0.055		
MMSE score	0.85 (0.69, 1.03)	0.103		
Apathy-related sub-network				
Local efficiency	0.03 (0.02, 0.04)	0.004		
Global efficiency	0.02 (0.01, 0.03)	<0.001	0.03 (0.01, 0.04)	0.007
Apathy-unrelated sub-network				
Local efficiency	0.03 (0.01, 0.04)	0.004		
Global efficiency	0.05 (0.02, 0.09)	0.007		
Whole brain network				
Local efficiency	0.02 (0.02, 0.03)	0.002		
Global efficiency	0.02 (0.01, 0.04)	0.001		

OR, odds ratio.

medial frontal gyrus, whose nodal degrees correlated negatively with the severity of apathy, as indicated in Table 2 and Fig. 2.

Cognitive aspects of apathy have been related to impairments in executive processes including holding information in working memory, planning and set-shifting [23]. Therefore, it might be expected that damage to parts of the executive network would be linked to apathetic symptoms. Indeed, our apathy-related network included the prefrontal cortex, a region whose damage has been linked to impairments of decision-making, shifting, rule finding and updating [24,25], thereby reducing goal-directed behavior. In addition to the frontal aspects of the executive network, regions in the posterior parietal lobe were also linked to apathy, including the right precuneus and right supramarginal gyrus. The precuneus is a well-known hub of the default-mode network and has been shown to be important for the manipulation of episodic memory, source memory, visuospatial information and consciousness [26]. The supramarginal gyrus has been linked to language processing and social judgement [27]. Dysfunction in these areas may be associated with apathy due to the deterioration of executive function and social cognition.

The aspects of apathy related to behavior may be associated with disruption to the prefrontal cortex-basal ganglia circuits. Damaged basal ganglia may fail to output relevant neural signals to targets in prefrontal cognitive and limbic territories [23,28]. In our study, it was found that the node in the right putamen was linked to apathy.

Several steps are needed to achieve goal-directed behavior, including the processing of external and internal cues, the elaboration of plans of action, task initiation, execution and feedback [23]. Apathy may arise from dysfunctions occurring at any of these steps. Within this process, integrating multisensory information, reorienting attention to relevant information and manipulating stimuli in working memory are also essential functions that are associated with the bilateral cingulate gyrus, bilateral superior temporal pole, right superior temporal gyrus, bilateral insula and occipital cortex [29,30] that were identified in our apathy-related network.

Our results reveal the involvement of a much larger apathy-related sub-network than previous hypotheses that considered lesion-induced disruption of frontal-subcortical circuits [3,23]. Therefore, apathy probably results not from dysfunction of a single circuit but from the decompensation of a more complicated sub-network.

Limitations and future studies

A few issues need to be addressed. First, deterministic DTI tractography was employed to reconstruct the whole brain networks. This method has shown a limited capacity for resolving crossing fiber bundles [14], and this typically leads to missed connections in the network (i.e. false negatives), which might have affected our findings. Future studies with more sophisticated tractography methods [31] and finer imaging techniques should be conducted to yield more accurate brain networks. Secondly, according to Stuss *et al*., post-stroke apathy patients can be categorized into emotional, cognitive or behavioral sub-syndromes [20]. Owing to the limited sample size, this method could not be used to categorize our participants. It would be intriguing in the future to reveal the sub-syndrome specific nodal dysfunction in the apathy network.

Conclusion

The present study used graph theoretical analysis of whole brain WM networks to identify an apathy-

related sub-network composed of 24 brain regions. The presence of apathy may not be due to the dysfunction of a single lesion or circuit but rather the decompensation of a complicated sub-network. These findings provide new insights into the neuroanatomical substrates of post-stroke apathy.

Acknowledgements

This work was supported by the 973 program (2013CB837300), the National Natural Science Foundation of China (Nos. 81000508, 81322021 and 81271649), the Beijing Nova Program (Z121110002512032) and the Pearl River Science and Technology Star Fund (2012J2200090).

Disclosure of conflicts of interest

The authors declare no financial or other conflicts of interest.

Supporting Information

Additional Supporting Information may be found in the online version of this article:

Table S1. Abbreviations.

References

1. Marin RS, Biedrzycki RC, Firinciogullari S. Reliability and validity of the Apathy Evaluation Scale. *Psychiatry Res* 1991; **38:** 143–162.
2. Van Dalen JW, Moll van Charante EP, Nederkoorn PJ, Van Gool WA, Richard E. Poststroke apathy. *Stroke* 2013; **44:** 851–860.
3. Jorge RE, Starkstein SE, Robinson RG. Apathy following stroke. *Can J Psychiatry* 2010; **55:** 350–354.
4. Okada K, Kobayashi S, Yamagata S, Takahashi K, Yamaguchi S. Poststroke apathy and regional cerebral blood flow. *Stroke* 1997; **28:** 2437–2441.
5. Hama S, Yamashita H, Yamawaki S, Kurisu K. Post-stroke depression and apathy: interactions between functional recovery, lesion location, and emotional response. *Psychogeriatrics* 2011; **11:** 68–76.
6. Le Bihan D. Looking into the functional architecture of the brain with diffusion MRI. *Nat Rev Neurosci* 2003; **4:** 469–480.
7. Crofts JJ, Higham DJ, Bosnell R, *et al*. Network analysis detects changes in the contralesional hemisphere following stroke. *Neuroimage* 2011; **54:** 161–169.
8. Yang SR, Hua P, Shang XY, *et al*. Predictors of early post ischemic stroke apathy and depression: a cross-sectional study. *BMC Psychiatry* 2013; **13:** 164.
9. Robert PH, Berr C, Volteau M, *et al*. Apathy in patients with mild cognitive impairment and the risk of developing dementia of Alzheimer's disease: a one-year follow-up study. *Clin Neurol Neurosurg* 2006; **108:** 733–736.
10. Jenkinson M, Smith S. A global optimisation method for robust affine registration of brain images. *Med Image Anal* 2001; **5:** 143–156.
11. Cui Z, Zhong S, Xu P, He Y, Gong G. PANDA: a pipeline toolbox for analyzing brain diffusion images. *Front Hum Neurosci* 2013; **7:** 42.
12. Tzourio-Mazoyer N, Landeau B, Papathanassiou D, *et al*. Automated anatomical labeling of activations in SPM using a macroscopic anatomical parcellation of the MNI MRI single-subject brain. *Neuroimage* 2002; **15:** 273–289.
13. Mori S, Crain BJ, Chacko VP, Van Zijl PC. Three-dimensional tracking of axonal projections in the brain by magnetic resonance imaging. *Ann Neurol* 1999; **45:** 265–269.
14. Mori S, Van Zijl PC. Fiber tracking: principles and strategies – a technical review. *NMR Biomed* 2002; **15:** 468–480.
15. Latora V, Marchiori M. Efficient behavior of small-world networks. *Phys Rev Lett* 2001; **87:** 198701.
16. He Y, Chen Z, Evans A. Structural insights into aberrant topological patterns of large-scale cortical networks in Alzheimer's disease. *J Neurosci* 2008; **28:** 4756–4766.
17. Humphries MD, Gurney K, Prescott TJ. The brainstem reticular formation is a small-world, not scale-free, network. *Proc Biol Sci* 2006; **273:** 503–511.
18. Xia M, Wang J, He Y. BrainNet Viewer: a network visualization tool for human brain connectomics. *PLoS One* 2013; **8:** e68910.
19. Liang Z, Zeng J, Liu S, *et al*. A prospective study of secondary degeneration following subcortical infarction using diffusion tensor imaging. *J Neurol Neurosurg Psychiatry* 2007; **78:** 581–586.
20. Stuss D, Van Reekum R, Murphy K. Differentiation of states and causes of apathy. In: Borod JC, ed. *The Neuropsychology of Emotion*. Oxford: Oxford University Press, 2000: 340–363. 19:598-609.
21. Rosen HJ, Hartikainen KM, Jagust W, *et al*. Utility of clinical criteria in differentiating frontotemporal lobar degeneration (FTLD) from AD. *Neurology* 2002; **58:** 1608–1615.
22. Elliott R, Newman JL, Longe OA, Deakin JF. Differential response patterns in the striatum and orbitofrontal cortex to financial reward in humans: a parametric functional magnetic resonance imaging study. *J Neurosci* 2003; **23:** 303–307.
23. Levy R, Dubois B. Apathy and the functional anatomy of the prefrontal cortex-basal ganglia circuits. *Cereb Cortex* 2006; **16:** 916–928.
24. Wallis JD. Orbitofrontal cortex and its contribution to decision-making. *Annu Rev Neurosci* 2007; **30:** 31–56.
25. Godefroy O. Frontal syndrome and disorders of executive functions. *J Neurol* 2003; **250:** 1–6.
26. Lundstrom BN, Ingvar M, Petersson KM. The role of precuneus and left inferior frontal cortex during source memory episodic retrieval. *Neuroimage* 2005; **27:** 824–834.
27. Silani G, Lamm C, Ruff CC, Singer T. Right supramarginal gyrus is crucial to overcome emotional egocentricity bias in social judgments. *J Neurosci* 2013; **33:** 15466–15476.
28. Laplane D, Levasseur M, Pillon B, *et al*. Obsessive-compulsive and other behavioural changes with bilateral basal ganglia lesions. A neuropsychological, magnetic

resonance imaging and positron tomography study. *Brain* 1989; **112**(Pt 3)**:** 699–725.
29. Koenigs M, Barbey AK, Postle BR, Grafman J. Superior parietal cortex is critical for the manipulation of information in working memory. *J Neurosci* 2009; **29:** 14980–14986.
30. Seghier ML. The angular gyrus: multiple functions and multiple subdivisions. *Neuroscientist* 2013; **19:** 43–61.
31. Behrens TE, Berg HJ, Jbabdi S, Rushworth MF, Woolrich MW. Probabilistic diffusion tractography with multiple fibre orientations: what can we gain? *Neuroimage* 2007; **34:** 144–155.